PHYSICAL REVIEW D **91,** 055015 (2015)

Distinguishing signatures of top- and bottom-type heavy vectorlike quarks at the LHC

Aarti Girdhar[*]

Department of Physics, Dr. B. R. National Institute of Technology, Jalandhar, India and Regional Centre for Accelerator-based Particle Physics, Harish-Chandra Research Institute, Chatnaag Road Jhunsi, Allahabad 211019, India

Biswarup Mukhopadhyaya[†]

Regional Centre for Accelerator-based Particle Physics, Harish-Chandra Research Institute, Chatnaag Road, Jhunsi, Allahabad 211019, India

Monalisa Patra[‡]

Department of Theoretical Physics, Tata Institute of Fundamental Research, Mumbai 400 005, India

(Received 25 April 2014; published 13 March 2015)

An SU(2) vectorlike singlet quark with a charge of either $+2/3(t')$ or $-1/3(b')$ is predicted in many extensions of the Standard Model. The mixing of these quarks with the top or bottom lead to flavor-changing Yukawa interactions and neutral currents. The decay modes of the heavier mass eigenstates are therefore different from the Standard Model-type chiral quarks. The LHC will provide an ideal environment to look for the signals of these exotic quarks. Considering all decays, including those involving Z and Yukawa interactions, we show how one can distinguish between t' and b' from ratios of event rates with different lepton multiplicities. The ability to reconstruct the Higgs boson with a mass around 125.5 GeV plays an important role in such differentiation.

DOI: 10.1103/PhysRevD.91.055015 PACS numbers: 12.60.-i, 14.80.Bn

I. INTRODUCTION

In spite of the enormous success of the Standard Model (SM) of particle physics in explaining experimental data, there are some sources of dissatisfaction. This encourages people to look beyond the SM (BSM).

Extending the particle content in, for example, the fermionic sector, is one of the ways of going beyond the SM. The presence of new chiral fermions (like the one predicted by fourth-generation theories) with couplings similar to the SM ones is strongly restricted by electroweak precision data [1]. Another possibility is the existence of vectorlike quarks, which was first motivated by the experimental measurement of the forward-backward asymmetry (A_b^{FB}) of the b quark [2] by the LEP experiments that showed about 2.9σ deviation from the value predicted by the best fit to the precision electroweak observables within the SM [3]. The existence of vectorlike quarks is also suggested by many BSM theories including the superstring-inspired E_6 models [4–7].

They also occur in other proposals, such as little Higgs theories [8,9] and extra-dimensional models [10]. Many of these scenarios also predict vectorlike leptons and extra gauge bosons. However, our focus in this paper will be on vectorlike quarks irrespective of any particular model. Depending on the context, these vectorlike quarks can be both top-like (charge $+2/3$) and bottom-like (charge $-1/3$) and can exist as triplets, doublets, or singlets under the $\mathrm{SU}(2)_L$ gauge group and hence have different hypercharges under $U(1)_Y$. The left- and right-handed components of the vectorlike quarks have the same quantum number under $\mathrm{SU}(3) \times \mathrm{SU}(2)_L \times U(1)_Y$, unlike the chiral SM.

(I) t'_L, $t'_R = (3, 1, 4/3)$ with electric charge $+2/3$, and mixes with t.

(II) b'_L, $b'_R = (3, 1, -2/3)$ with electric charge $-1/3$, and mixes with b.

The collider phenomenology of these vectorlike isosinglets has been considered extensively in the literature (for the most recent studies, see Refs. [11–25]). We consider the possibility of vectorlike isosinglet quarks in both sectors, taking one at a time in addition to the three generations of SM chiral fermions. The inclusion of a weak isospin singlet fermion leads to mixing between the singlet fermions and the SM doublets and hence different phenomenological consequences from that predicted by the SM. The aim of our work is to distinguish between the top- and bottom-type (t' and b') singlets from their decays. In particular, we wish to utilize the fact that flavor-changing decays into the Higgs are possible. The mass of the Higgs is now known, thanks to its recent discovery at the LHC experiments [26,27]. We make use of this fact and tag five b's along with the requirement of two b pairs giving invariant mass peaks at

[*]aarti@hri.res.in
[†]biswarup@hri.res.in
[‡]monalisa@theory.tifr.res.in

m_H for both of the isosinglets. The general method has been to choose events with a final state of W/Z bosons and jets consistent with the decay of the heavy quarks. We find that we can distinguish between the t' and the b' from the ratio of events, with final states of different lepton multiplicities.

The outline of the paper is as follows. In Sec. II, we discuss the couplings of the t' and b' to the SM fields separately in a model-independent way using the effective Lagrangian. In Sec. III, we discuss the signal and background along with the methodology adopted for the analysis of the signal. In Sec. IV, the results of our numerical analysis based on Monte Carlo simulations are presented. We summarize and conclude in Sec. V.

II. PHENOMENOLOGY OF t' AND b'

Strong processes can produce both t'- and b'-type quarks at the LHC with identical rates, through gluon fusion or quark-antiquark annihilation. Such pair production processes (whose rates are independent of the degree of singlet-doublet mixing) are the relevant modes for our study. Though single production is also possible (perhaps with less phase-space suppression), it is (a) driven by electroweak couplings, and (b) suppressed by the singlet-doublet mixing angle(s). The dominant decays of t' and b' are expected to be as follows:

(1) $t' \to W^+ b$, $t' \to Ht$, $t' \to Zt$;
(2) $b' \to W^- t$, $b' \to Hb$, $b' \to Zb$.

A. Mixing and coupling of t' and b'

We assume that the vector quark only mixes with the third generation of quarks. We show below the general scheme of mixing in the down sector; the pattern is similar in the up sector as well. The weak eigenstates are related to the mass eigenstate by [28,29]

$$\begin{pmatrix} d_w \\ s_w \\ b_w \\ b'_w \end{pmatrix} = U \begin{pmatrix} d \\ s \\ b \\ b' \end{pmatrix},$$

$$U_{4\times4} = \begin{pmatrix} V_{3\times4} \\ X_{1\times4} \end{pmatrix} = \begin{pmatrix} V_{ud} & V_{us} & V_{ub} & V_{ub'} \\ V_{cd} & V_{cs} & V_{cb} & V_{cb'} \\ V_{td} & V_{ts} & V_{tb} & V_{tb'} \\ X_{4d} & X_{4s} & X_{4b} & X_{4b'} \end{pmatrix}. \tag{2.1}$$

The unprimed fields denote the basis where the mass matrix of the up-type quarks are diagonalized. $V_{3\times4}$ is the charged-current matrix analogous to the SM Cabibbo-Kobayashi-Maskawa (CKM) matrix and is not unitary. The addition of the fourth row makes $U_{4\times4}$ unitary. The charged-current interaction in the mass basis is given by

$$\mathcal{L}_{\rm CC} = \frac{e}{2\sqrt{2}\sin\theta_W}[\bar{u}^i_L \gamma^\mu V_{ij} d^j_L] W^+_\mu + \text{H.c.}, \tag{2.2}$$

where e is the electromagnetic coupling constant, θ_W is the weak mixing angle, and $V_{ij}(i = 1, 3, j = 1, 4)$ is the relevant 3×4 submatrix of U. As a consequence of mixing between fields with different weak isospin (T_3), flavor-changing neutral-current (FCNC) processes appear at the tree level, something that is absent in the SM framework. We therefore get $b'bZ$ and $b'bH$ interactions. The neutral-current interaction in the mass basis is given by

$$\mathcal{L}_{NC} = \frac{e}{2\sin 2\theta_W}[\bar{u}^k_L \gamma^\mu u_{kL} - \bar{d}^i_L \gamma^\mu (V^\dagger V)_{ij} d^j_L - 2\sin^2\theta_W J^\mu_{em}] Z_\mu, \tag{2.3}$$

where $k = 1, 3$ and $i,\ j = 1, 4$. The electromagnetic current J^μ_{em} is diagonal in the mass basis and is

$$J^\mu_{em} = \frac{2}{3}\bar{u}^k \gamma^\mu u_k - \frac{1}{3}\bar{d}^i \gamma^\mu d_i. \tag{2.4}$$

The FCNC coupling as seen from Eq. (2.3) is controlled by $V^\dagger V$, which is a 4×4 matrix. Since the mixing matrix $V_{3\times4}$ is embedded within the unitary matrix, from Eq. (2.1) we obtain the relation

$$(V^\dagger V)_{ij} = \delta_{ij} - U^*_{i4} U_{j4}. \tag{2.5}$$

On account of the nonchiral nature of the vector quarks in the current scenario, the SU(2) singlet field b' can have gauge-invariant "bare" mass terms proportional to $\bar{b}'_L b'_R$ and $\bar{b}'_L f'_R [f' = (d,\ s,\ b)]$, contrary to d, s, and b. As these terms do not arise from the Yukawa coupling, the Yukawa matrix cannot be simultaneously diagonalized with the mass matrix, consequently giving rise to nondiagonal Yukawa couplings among the physical quarks. The relations are analogous for the top sector.

The nonobservation of the FCNC decays in the top sector by the Tevatron [30] and the analysis of single top production at LEP [31] have set bounds on the CKM matrix elements involving the top quark at 95% C.L. The limits on the allowed mass range and mixing angle θ were presented in Ref. [32] according to the precision electroweak data, flavor physics, and oblique parameters. For our analysis we have assumed the following simplified version of the matrix given in Eq. (2.1):

$$U = \begin{pmatrix} V_{ud} & V_{us} & V_{ub} & 0 \\ V_{cd} & V_{cs} & V_{cb} & 0 \\ V_{td} & V_{ts} & \cos\theta & \sin\theta \\ 0 & 0 & -\sin\theta & \cos\theta \end{pmatrix}. \tag{2.6}$$

We are essentially considering the case where the isosinglet quark in either sector mixes only with the third

family and the mixing angle is consistent with all existing constraints.

The current phenomenological constraints on vectorlike quarks come from direct-production bounds at the various colliders,

(i) The CDF [33,34], ATLAS [35–39], and CMS [40] collaborations have set a lower limit on exotic quark masses with charge $+2/3$ and $-1/3$ by investigating either a particular decay channel or by assuming branching ratios to W, Z, and H decay modes in the context of different models.

(ii) The CMS Collaboration [41] reported the latest limit on the mass of t' (assuming strong production) at 95% C.L. and $\sqrt{s} = 8$ TeV as being between 687 and 782 GeV for different values of the branching ratios into the three different final states. We consider all the possible decay modes of the heavy quarks and take this limit for our analysis.

Flavor constraints are also significant for vectorlike quarks. The nonunitarity of the SM CKM matrix is tightly constrained by the precision measurement of the unitarity triangle of the SM. The FCNC leads to some processes, such as $b \to s\gamma$ (b changes its flavor by emitting or absorbing a Z/H boson) and b-meson mixing (e.g., $B_d - \bar{B}_d$ and $B_s - \bar{B}_s$ mixing) [32,42]. The experimental data from this sector can be applied to find constraints on the heavy quarks and their mixing with the SM ones. However, we do not consider such constraints for our analysis as they are largely model dependent [43,44]. We present in Fig. 1 the cross section of the vectorlike quark pair production at the 14 TeV LHC. The production cross section decreases with the mass of the vector quarks and is independent of the mixing angle θ. Moreover, the cross section is the same for the two cases considered here. Figure 2 shows the branching ratios of the various decay modes of the vector quarks in the two cases, plotted as functions of their mass. The Higgs mass is kept fixed at $m_H = 125.5$ GeV. These branching ratios are sensitive to the Higgs mass and have a very weak dependence on θ. Hence, we present our results for a fixed value of θ.

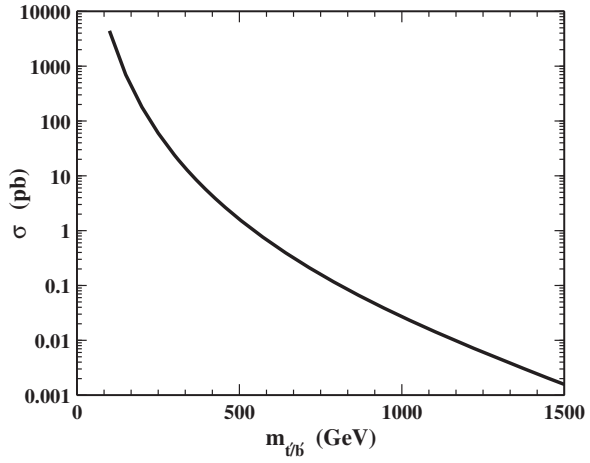

FIG. 1. The pair production cross section of t' and b' as a function of mass for a mixing angle $\theta = 5$ at the 14 TeV LHC.

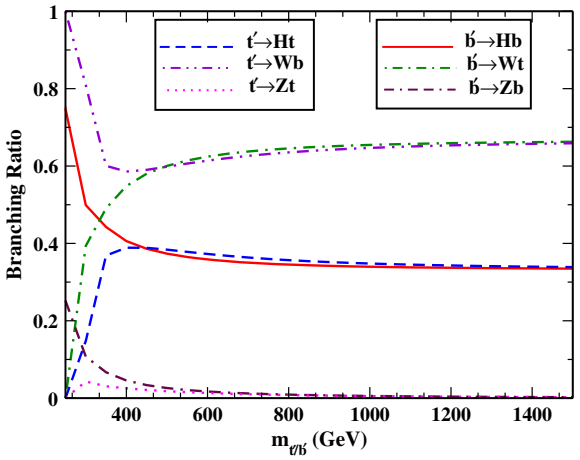

FIG. 2 (color online). The branching ratios for the vectorlike quarks t' and b' as a function of mass for a fixed mixing angle $\theta = 5$.

III. SIGNAL AND BACKGROUNDS

We consider (as already mentioned) the pair production of both $t'\bar{t}'$ and $b'\bar{b}'$, taking one at a time via quark-antiquark and gluon pair annihilation. The recent discovery of the Higgs with a mass around 125–126 GeV provided an added edge, given the fact that the Higgs dominantly decays to $b\bar{b}$ in this mass range. Thus, it is helpful to look at $5b$ events, with a pair of b's peaking close to the Higgs mass. The fact that (for the allowed range of the mixing matrix elements) the branching fractions of t' or b' to a Higgs is substantial for moderate masses lends confidence to this proposal.

A. Signal

t'—We will be mainly concentrating on the decay mode of t' to a Higgs and a top quark: $pp \to t'\bar{t}' \to HtH\bar{t} \to b\bar{b}W^+bb\bar{b}W^-\bar{b}$.

In this case there are three possible outcomes depending on the decay modes of both of the W's: (i) both of the W's decay to leptons, (ii) one of the W's decays leptonically and the other decays hadronically, or (iii) both of the W's decay hadronically. Thus the final states arising from $t'\bar{t}'$ production are

(a) $6b + 2l + \not{p}_T$(leptonic),
(b) $6b + 1l + \not{p}_T + 2$ jets (semi leptonic), and
(c) $6b + 4$ jets (hadronic).

The same final states can also be obtained from other decay modes of t'. The processes that mimic the $t'\bar{t}'$ decay channel considered for our analysis are

(a) $pp \to t'\bar{t}' \to ZtZ\bar{t} \to b\bar{b}W^+bb\bar{b}W^-\bar{b}$, and
(b) $pp \to t'\bar{t}' \to ZtH\bar{t}/HtZ\bar{t} \to b\bar{b}W^+bb\bar{b}W^-\bar{b}$.

The contribution from these decay channels is proportional to the branching ratio of $Z \to b\bar{b}$, which is close to 15% and

thus is too small. It must be remarked that (when added to the small branching ratio) their contribution to the signal gets filtered by the various cuts and the calculation of the Higgs invariant mass, as explained later.

b'—In this case the decay mode of interest is also $b' \to bH$, leading to a final state consisting of six b's: $pp \to b'\bar{b}' \to HbH\bar{b} \to b\bar{b}b\bar{b}b\bar{b}$.

There are other modes for b' which can give rise to such b multiplicities. Of course, the contributions from all these processes are proportional to the respective branching fractions of $Z \to b\bar{b}$:

(a) $pp \to b'\bar{b}' \to ZbZ\bar{b} \to b\bar{b}b\bar{b}b\bar{b}$,
(b) $pp \to b'\bar{b}' \to ZbH\bar{b}/HbZ\bar{b} \to b\bar{b}b\bar{b}b\bar{b}$.

For both t' and b', we look for the following final-state signals, mainly with five tagged b's that reconstruct two Higgs in the mass range 123–128 GeV:

Signal 1: $5b + 2l + \not{p}_T$,
Signal 2:$5b + 1l + \not{p}_T$,
Signal 3:$5b$.

We get leptons in the $b'\bar{b}'$ production channel from the decay modes $b' \to bZ$ and $b' \to tW$ and the combinatorics, in spite of the fact that our channel of interest gives a final state of six b's only. The package CALCHEP v2.5.6 [45] is used to calculate the cross section for the signal process and the respective branching ratios of t' and b'.

B. Backgrounds

There are many SM processes that can fake the signals listed above. The dominant backgrounds arise from

(1) $pp \to t\bar{t}HH$,
(2) $pp \to t\bar{t}H + 2$ jets,
(3) $pp \to t\bar{t} + \mathrm{N}$ jets, where $0 \le \mathrm{N} \le 4$,
(4) $pp \to t\bar{t}b\bar{b} + \mathrm{N}$ jets, where $0 \le \mathrm{N} \le 2$, and
(5) $pp \to W^+W^-HH + \mathrm{N}$ jets, where $0 \le \mathrm{N} \le 2$.

We have computed the cross section for all the background processes (except the process $pp \to t\bar{t}HH$) with ALPGEN [46], which takes into account all the spin correlation and finite-width effects. The cross section for the production of $t\bar{t}HH$ is computed with CALCHEP v2.5.6 [45], and is found to be about 0.0005 pb at 14 TeV for a Higgs mass of 125.5 GeV. Since it is too small to be a threat to our signal, we are not considering this process further in our analysis. A similar argument follows for the background production of W^+W^-HH in association with jets. The cross section is of the order of 10^{-5} pb. Therefore we are also ignoring this process in our analysis of the background. The QCD factorization and renormalization scale (Q^2) in ALPGEN for the different background processes are presented in Table I.

TABLE I. The factorization and renormalization scale (Q^2) considered for the different background channels in ALPGEN.

Process	Q^2
$pp \to t\bar{t}H$	$(2m_t + 2m_H)^2$
$pp \to t\bar{t}$	m_t^2
$pp \to t\bar{t}b\bar{b}$	m_t^2
$pp \to W^+W^-HH$	$m_W + m_H$

1. Event selection criteria

Our task is two-fold. First, we need to reduce the SM backgrounds to signals 1, 2, and 3 listed above. Next, we need to see how the ratios of event rates in different channels (after applying the event selection criteria) differ between the two cases of t' and b' pair production. We have used the CTEQ6L parton distribution function with $m_t = 172$ GeV, $m_b = 4.8$ GeV, $m_H = 125.5$ GeV, and a center-of-mass energy $\sqrt{s} = 14$ TeV for our numerical evaluation. The signal events along with their decay branching fractions are generated with the help of CALCHEP v2.5.6 [45]. The renormalization and factorization scale used for the calculation of production cross sections is the default scale used in CALCHEP, i.e., the squared subprocess center-of-mass energy $[m_{ij}{}^2 = \hat{s} = (p_i + p_j)^2]$. These signal events are passed on to PYTHIA 6.4.24 [47] for showering and hadronization along with the help of the CALCHEP-PYTHIA interface program [48]. In PYTHIA, we have taken into account the initial- and final-state radiations due to QED and QCD, along with the multiple interactions accounting for pileup. The showering of the SM background events is done by passing the output of ALPGEN [46] (in the form of unweighted events) to PYTHIA. ALPGEN performs the matching of the jets produced in the showering routine to the partons obtained from the matrix-element calculation using the MLM matching procedure [49]. Jet formation is done in FASTJET 3.0.2 [50] using the anti-k_t algorithm, with radius parameter $R = 0.4$. The event selection criteria and the cuts applied are the same for both the signal and the background, and are detailed below.

(1) Identification of isolated leptons (cut 1):
   (a) For the lepton trigger, electron candidates are required to have $p_T^e > 25$ GeV and $|\eta| < 2.47$. Moreover, the electron is vetoed if it lies in the region $1.37 < |\eta| < 1.52$ between the barrel and end-cap electromagnetic calorimeters. The muons are required to satisfy $p_T^\mu > 25$ GeV and $|\eta| < 2.5$.
   (b) Since we are interested in leptons coming from the decay of on-shell W's only, they are further tested to determine whether they are isolated.
      (i) The total E_T of stable particles within the cone radius of the lepton $[\Delta R = \sqrt{(\Delta\eta)^2 + (\Delta\phi)^2} < 0.2]$ should be less than 10 GeV.
      (ii) In order to ensure that the lepton and jets are well separated, we further apply a lepton jet separation cut, $\Delta R_{lj} \ge 0.4$, on the lepton for all the jets formed with $p_T > 20$ GeV. The jets are formed in FASTJET [50]

TABLE II. Actual number of events that pass various cuts in the case of the signal and background for a $5b + 2l + \not{p}_T$ final state at the 14 TeV LHC.

Actual number of events with $\mathcal{L} = 1000$ fb^{-1}							
$m_{t',b'}$ (GeV)	Process	At prod.	cut 1	cut 2	cut 3	NH ≥ 1	NH $= 2$
500	$t'\bar{t}'$	1.60×10^6	4.92×10^4	4.05×10^4	747	187	16.1
	$b'\bar{b}'$	1.61×10^6	8.09×10^4	7.35×10^4	61.2	14.1	1
700	$t'\bar{t}'$	2.40×10^5	6.58×10^3	6.21×10^3	148	29.3	3.42
	$b'\bar{b}'$	2.40×10^5	1.85×10^4	1.76×10^4	9.4	1.39	.116
800	$t'\bar{t}'$	1.09×10^5	2.90×10^3	2.78×10^3	64.86	12.82	1.26
	$b'\bar{b}'$	1.08×10^5	6.10×10^3	5.84×10^3	5.4	0.96	0.06
	$t\bar{t}H + 2$ jets	1.57×10^5	5.06×10^3	4.09×10^3	7.01	0	0
Background	$t\bar{t}b\bar{b} + 2$ jets	2.74×10^5	5.27×10^3	4.27×10^3	28	6	0.6
	$t\bar{t} + 4$ jets	1.74×10^7	3.46×10^5	2.80×10^5	0	0	0

(with $R = 0.4$) using the anti-k_t jet algorithm. All the particles other than the leptons with a trigger of $p_T > 20$ GeV and $|\eta| < 2.5$ form the input for FastJet. The jets trigger for this is $p_T > 20$ GeV. The events chosen after this are listed as passing cut 1 for the one-lepton case (signal 2).

(iii) For the case where we require two isolated leptons (signal 1), in order to avoid the same-flavor leptons that might come from the decay of a Z boson, the invariant mass M_{ll} of the isolated lepton pairs is calculated and the pair having a mass in the window $|M_Z \pm 10|$ GeV is discarded. The events chosen after this are listed as passing cut 1.

(2) Missing E_T ($\not{E}_T$) (cut 2): For the events with one or two isolated leptons, $\not{E}_T$ is calculated by computing the vector sum of the visible $p_T^{\rm tot}$ of all particles, where

$$\begin{aligned} \vec{\not{E}}_T &= -\Sigma \vec{p}_T^{\,\rm tot}, \\ p_T^{\rm tot} &= \sqrt{(p_x^{\rm tot})^2 + (p_y^{\rm tot})^2}, \\ p_x^{\rm tot} &= p_x^{e^\pm} + p_x^{\mu^\pm} + p_x^{\rm jets} + p_x^{\rm unc} \\ p_y^{\rm tot} &= p_y^{e^\pm} + p_y^{\mu^\pm} + p_y^{\rm jets} + p_y^{\rm unc}. \end{aligned} \tag{3.1}$$

In Eq. (3.1), $p_{x,y}^{\rm unc}$ receives contributions from the unclustered components, which consist of the leptons and hadrons in each event that do not pass the primary selection criteria for the trigger, but that have $p_T > 0.5$ and $|\eta| < 5.0$. A cut of $\not{E}_T > 40$ GeV (referred to as cut 2) is applied. All the events that survive cut 1 are subjected to this cut.

(3) b tagging (cut 3): The jets with $E_T > 40$ GeV and $|\eta| < 2.5$ are selected as a trigger for the identification of b jets. A jet is tagged as a b jet if it has a b parton within a cone of $\Delta R < 0.4$ with the jet axis, and a tagging efficiency of 60% is incorporated. Events with five or more b's tagged in this manner are selected and are tabulated as events surviving cut 3.

(4) Invariant mass reconstruction: For the events with at least five tagged b's (i.e., those that survive cut 3), the invariant masses m_{bb} of all possible b-jet pairs are computed, and those with m_{bb} in the mass range 123 GeV $\leq m_H \leq$ 128 GeV are considered to be coming from the decay of a Higgs. In Tables II, III, and IV, the column labeled "NH ≥ 1" represents the number of events which have at least one b pair in the given Higgs mass range, and the column labeled "NH $= 2$" represents the number of events with two b pairs within the required Higgs mass

TABLE III. Actual number of events that pass various cuts in the case of the signal and background for a $5b + 1l + \not{p}_T$ final state at the 14 TeV LHC.

Actual number of events with $\mathcal{L} = 1000$ fb^{-1}							
$m_{t',b'}$ (GeV)	Process	At prod.	cut 1	cut 2	cut 3	NH ≥ 1	NH $= 2$
500	$t'\bar{t}'$	1.60×10^6	4.23×10^5	4.26×10^5	9.28×10^3	2.28×10^3	333
	$b'\bar{b}'$	1.61×10^6	4.19×10^5	3.54×10^5	799	182	35.3
700	$t'\bar{t}'$	2.40×10^5	6.33×10^4	5.67×10^4	1.91×10^3	441	40
	$b'\bar{b}'$	2.40×10^5	7.78×10^4	7.01×10^4	151	27.62	1.59
800	$t'\bar{t}'$	1.08×10^5	2.84×10^4	2.59×10^4	890	188	18.75
	$b'\bar{b}'$	1.08×10^5	2.95×10^4	2.70×10^4	108	10.89	1.1
	$t\bar{t}H + 2$ jets	1.57×10^5	4.2×10^4	3.3×10^4	175	45.5	0
Background	$t\bar{t}b\bar{b} + 2$ jets	2.74×10^5	6.59×10^4	4.75×10^4	392	83.7	12.1
	$t\bar{t} + 4$ jets	1.78×10^7	4.37×10^6	3.18×10^6	1.18×10^3	238	238

TABLE IV. Actual number of events surviving after various cuts in the case of the signal and background for a $5b + 0l$ final state with two b pairs giving an invariant mass peak at the 14 TeV LHC.

		Actual number of events with $\mathcal{L} = 1000$ fb^{-1}			
$m_{t',b'}$ (GeV)	Process	At prod.	cut 3	NH ≥ 1	NH $= 2$
500	$t'\bar{t}'$	1.6×10^6	3.74×10^4	9.67×10^3	1.35×10^3
	$b'\bar{b}'$	1.61×10^6	6.88×10^4	1.23×10^4	1.10×10^3
700	$t'\bar{t}'$	2.39×10^5	6.85×10^4	1.51×10^3	139
	$b'\bar{b}'$	2.39×10^5	7.83×10^3	188	49.69
800	$t'\bar{t}'$	1.08×10^5	3.2×10^3	652	54.07
	$b'\bar{b}'$	1.08×10^5	4.8×10^4	678	35.2
Background	$t\bar{t}H + 2$ jets	1.57×10^5	865	266	38.5
	$t\bar{t}b\bar{b} + 2$ jets	2.74×10^5	1.94×10^3	427	57.8
	$t\bar{t} + 4$ jets	1.78×10^7	7.36×10^3	1.19×10^3	0

range. The numbers listed in the "NH $= 2$" column represent N_i, with $i = 1, 2, 3$ (described in detail in Sec. III), and are used to get the desired ratios.

The cuts mentioned above are mainly motivated to suppress the background and also to discriminate the signals of the t' and b'.

2. Smearing

In order to account for detector effects, the momenta of the leptons, jets, and the unclustered components obtained from the generator are smeared according to the following prescription.

(i) For electrons and jets: The electrons with pseudorapidity $|\eta| < 2.5$ and the jets with $|\eta| < 5$ and $p_T > 20$ GeV are smeared by a Gaussian distribution, given by

$$\frac{\sigma(X)}{X} = \frac{a}{\sqrt{X}} \oplus b \oplus \frac{c}{X}, \tag{3.2}$$

where X $= E_T$. In the case of the electrons,

$$(a, b, c) = \begin{pmatrix} (0.030\ \text{GeV}^{1/2}, 0.005, 0.2\ \text{GeV}) & |\eta| < 1.5 \\ (0.055\ \text{GeV}^{1/2}, 0.005, 0.6\ \text{GeV}) & 1.5 < |\eta| < 1.5 \end{pmatrix}, \tag{3.3}$$

whereas for the jets $a = 0.5$ GeV$^{1/2}$, and $b = c = 0$.

(ii) For muons: Muons with $|\eta| < 2.5$ are similarly smeared according to

$$\frac{\sigma(p_T)}{p_T} = \begin{pmatrix} a, & p_T < 100\ \text{GeV} \\ a + b log\frac{p_T}{100\ \text{GeV}}, & p_T > 100\ \text{GeV} \end{pmatrix}, \tag{3.4}$$

with

$$(a, b) = \begin{pmatrix} (0.008, 0.037) & |\eta| < 1.5 \\ (0.020, 0.050) & 1.5 < |\eta| < 1.5 \end{pmatrix}. \tag{3.5}$$

(iii) For unclustered components: The stable particles with $|\eta| < 5.0$ and $E_T > 0.5$ GeV are smeared as unclustered components, and the corresponding Gaussian width is

$$\sigma(E_T) = \alpha\sqrt{\Sigma_i E_T^{(\text{unc})_i}}, \tag{3.6}$$

with $\alpha \approx 0.55$. In this case the x and y components of E_T^{unc} are smeared independently by the same quantity.

IV. NUMERICAL RESULTS

In Sec. III we briefly discussed the final-state signal along with the various cuts applied for our analysis. We present in this section the actual number of events surviving after each cut for a given integrated luminosity of 1000 fb^{-1}. In Tables II, III, and IV, we present the rates for various lepton multiplicities for two masses of both t' and b', associated with the existing limits. We also present the numbers for $m_{t'} = m_{b'} = 500$ GeV in order to illustrate the results.

(i) First, we define N_1 as the number of events with the final state $5b + 2l + \not{p}_T$ (signal 1), i.e., five tagged b jets with the invariant mass of two b-jet pairs peaking at the Higgs mass (123–128 GeV) along with two isolated leptons. The number of events surviving after each cut for this final state (for the considered integrated luminosity) is presented in Table II for both the signal and background processes.

(ii) Next, we define N_2 as the number of events with at least five tagged b's and one isolated lepton, i.e., $5b + 1l + \not{p}_T$ (signal 2) in the final state, along with the invariant mass of two b-jet pairs peaking at the Higgs mass (123–128 GeV). We present the results for this final state in Table III for both t' and b' along with the background. The argument in this case for the number of events surviving after each cut is similar to the previous one. The events that survive even after the Higgs invariant mass reconstruction in the case of backgrounds are mainly due to the combinatorics.

(iii) Finally, we define N_3 as the number the events with at least five tagged b jets and zero leptons (signal 3), along with the invariant mass of two b-jet pairs peaking at the Higgs mass (123–128 GeV). The results for this are presented in Table IV for both t' and b'. While considering the zero-lepton final state given in Table IV, the cuts consisting of an isolated lepton and missing energy, i.e., cuts 1 and 2 are neglected for obvious reasons. Since both t' and b' favor the hadronic decay mode (as can be seen from Table IV) the number of events surviving is the same even after cut 3. It is only after the Higgs mass reconstruction from the b jets that both t' and b' show different behavior.

From the above analysis, we find a significant difference in the number of events that survive after all the cuts for both of the signals. It can be seen from Tables II, III, and IV that it is only after cut 3 (tagging five b's) and not cut 2 (missing E_T) that the difference in the t' and b' signals starts to appear. This happens because the dominant decay mode of b' is tW, and hence the final state of b' will also have a large amount of missing E_T. We compute the ratios of the number of events surviving after the application of all cuts for each of the three signals, $N_i (i = 1, 2, 3)$, as defined before for both t' and b'. The relevant ratios that we consider are $N_{13} = N_1/N_3$ and $N_{23} = N_2/N_3$ for both t' and b'. We consider these ratios because working with the above rates allows us to cancel most of the systematic uncertainties. The results are presented in Table V. We can make the following observations.

(i) When t' and b' have the same mass, N_{13} differs by a factor of 10.

TABLE V. The ratios N_{13} and N_{23} for t' and b'.

Mass (GeV)	Isosinglet	N_{13}	N_{23}
500	t'	0.012	0.246
	b'	0.0009	0.032
700	t'	0.025	0.29
	b'	0.002	0.032
800	t'	0.02	0.35
	b'	0.002	0.03

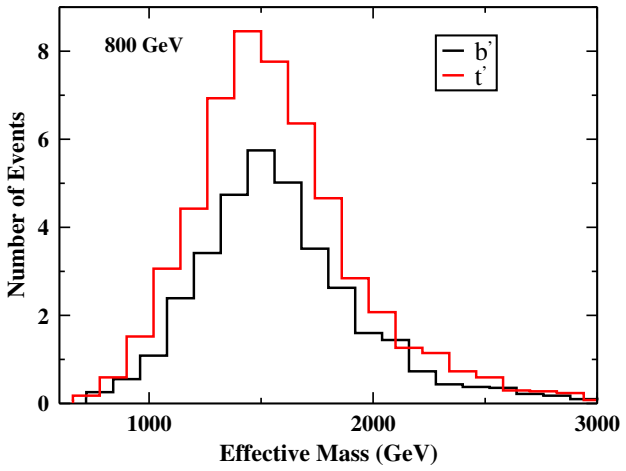

FIG. 3 (color online). The effective mass distribution for $m_{t'} = m_{b'} = 800$ GeV for a mixing angle $\theta = 5$ at the 14 TeV LHC, in the $5b + 0l$ final state.

(ii) When t' and b' have the same mass, N_{23} differs by a factor of 10.

(iii) In principle, it can be argued that the distinction in terms of the event ratios is not conclusive: the values of N_{13} and N_{23} for one $m_{t'}$ may be the same as those of another $m_{b'}$. Such ambiguity can be removed from the simultaneous study of the effective mass distributions of the events, where the effective mass is defined as $M_{\text{eff}} = \Sigma p_T^{\text{visible}} + \Sigma p_T^{\text{missing}}$. As can be seen from Figs. 3, 4, and 5, the M_{eff} distributions in the pair production of either t' or b' exhibit a peak at $2m_{t'}$ $(2m_{b'})$. Thus, once the exotic quark mass is indicated from the M_{eff} distribution, the values of N_{13} and N_{23} enable us to differentiate t' from b' without the aforementioned ambiguity, and the distinction is rather obvious, as can be seen in Fig. 6.

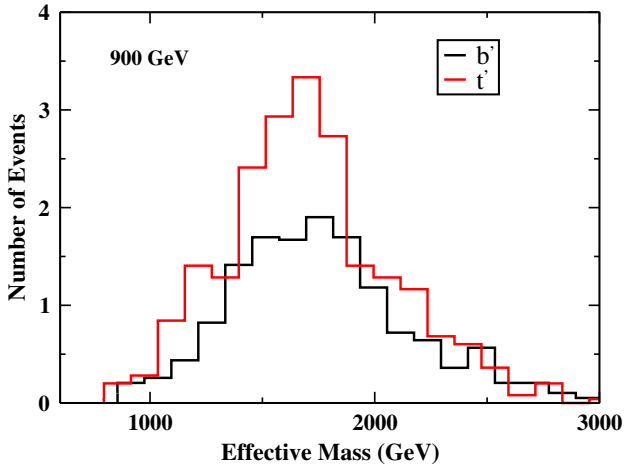

FIG. 4 (color online). The effective mass distribution for $m_{t'} = m_{b'} = 900$ GeV for a mixing angle $\theta = 5$ at the 14 TeV LHC, in the $5b + 0l$ final state.

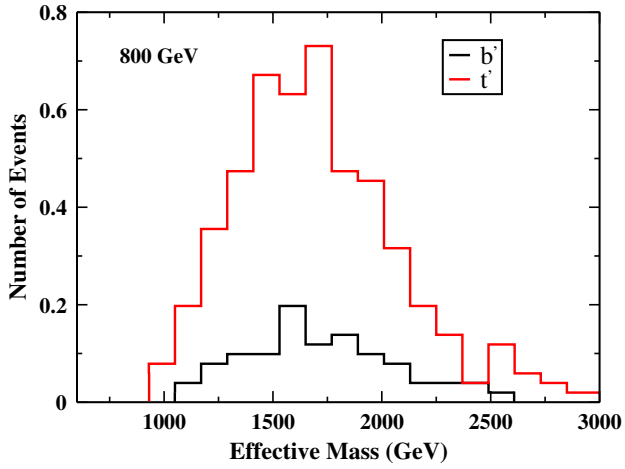

FIG. 5 (color online). The effective mass distribution for $m_{t'} = m_{b'} = 800$ GeV for a mixing angle $\theta = 5$ at the 14 TeV LHC, in the $5b + 1l + \not{p}_T$ final state.

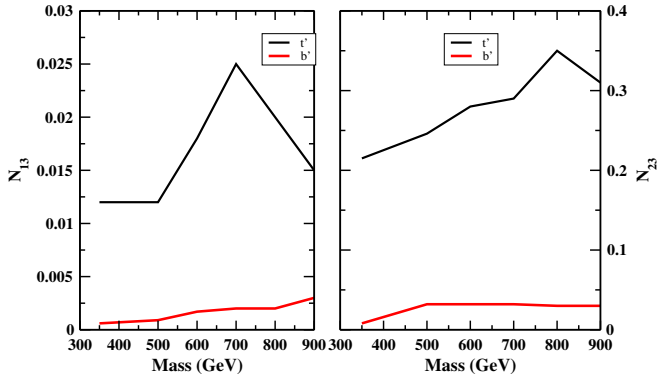

FIG. 6 (color online). The ratios N_{13} and N_{23} as functions of the masses of t' and b'.

Therefore, we conclude that the ratios N_{13} and N_{23} can be used to discriminate the signals for t' and b' when both t' and b' decay to a Higgs and the respective third-generation partner. The ratios N_{13} and N_{23} as functions of the masses of t' and b' are shown in Fig. 6.

V. SUMMARY AND CONCLUSIONS

In this work, we have made an attempt to distinguish between top-like and bottom-like isosinglet quarks—which are predicted in several extensions of the SM—at a luminosity of 1000 fb^{-1} and a center-of-mass energy of 14 TeV at the LHC. Because they are vectorlike, they mix with third-generation chiral quarks, which leads to flavor-changing Yukawa interactions along with FCNCs. These quarks have the decay modes $t' \to Zt$, Ht, W^+b, and $b' \to Zb$, Hb, W^-t. In this work we have tried to address the problem of distinguishing the signatures of these isosinglet vectorlike quarks once they are discovered.

In particular, we chose the Higgs decay channel for both t' and b', and we tried to make a distinction between the two cases. The Higgs decays further to a pair of b quarks. We demanded that the two Higgs be reconstructed in the mass range 123–128 GeV from the tagged b's. The recent discovery of a Higgs-like resonance at 125.5 GeV at the LHC strengthens our analysis. We chose three final states with two, one, and zero leptons along with five tagged b's, which is attainable at the LHC as it can efficiently detect leptons and also tag b's. We find that with a suitable choice of cuts, the SM background is very small for both of the signals. Our study overall reveals that—empowered by our recent information on the Higgs—we can clearly differentiate between t' and b' from ratios of events with various lepton multiplicities in the final state along with two reconstructed Higgs.

ACKNOWLEDGMENTS

A. G. is thankful to Department of Science and Technology, New Delhi for the grant (No. SR/WOS-A/PS-04/2009) under Women in Science scheme. B. M. acknowledges the funding available from the Department of Atomic Energy, Government of India, for the Regional Centre for Accelerator based Particle Physics (RECAPP), Harish-Chandra Research Institute. M. P. would like to extend her thanks to RECAPP for the local hospitality and computational assistance during the course of this work.

[1] S. Chatrchyan *et al.* (CMS Collaboration), Phys. Rev. D **86**, 112003 (2012).
[2] M. S. Chanowitz, Phys. Rev. Lett. **87**, 231802 (2001).
[3] G. Alexander *et al.* (LEP, ALEPH, and DELPHI Collaborations), Phys. Lett. B **276**, 247 (1992).
[4] I. Gogoladze, B. He, and Q. Shafi, Phys. Lett. B **690**, 495 (2010).
[5] S. Dawson and E. Furlan, Phys. Rev. D **86**, 015021 (2012).
[6] V. D. Barger, N. Deshpande, R. J. N. Phillips, and K. Whisnant, Phys. Rev. D **33**, 1912 (1986); Phys. Rev. D **35**, 1741(E) (1987).
[7] M. Cvetic, J. Halverson, and P. Langacker, J. High Energy Phys. 11 (2011) 058.
[8] N. Arkani-Hamed, A. G. Cohen, E. Katz, A. E. Nelson, T. Gregoire, and J. G. Wacker, J. High Energy Phys. 08 (2002) 021.

[9] N. Arkani-Hamed, A. G. Cohen, E. Katz, and A. E. Nelson, J. High Energy Phys. 07 (2002) 034.
[10] H. C. Cheng, B. A. Dobrescu, and C. T. Hill, arXiv:hep-ph/0004072.
[11] B. Mukhopadhyaya, A. Ray, and A. Raychaudhuri, Phys. Lett. B **186**, 147 (1987).
[12] F. del Aguila, L. Ametller, G. L. Kane, and J. Vidal, Nucl. Phys. **B334**, 1 (1990).
[13] F. del Aguila, J. A. Aguilar-Saavedra, and R. Miquel, Phys. Rev. Lett. **82**, 1628 (1999).
[14] F. del Aguila and J. A. Aguilar-Saavedra, *Proc. Sci. Corfu.* 98 (1998) 020.
[15] J. A. Aguilar-Saavedra, Phys. Lett. B **625**, 234 (2005); Phys. Lett. B **633**, 792(E) (2006).
[16] J. A. Aguilar-Saavedra, J. High Energy Phys. 11 (2009) 030.
[17] B. Bhattacherjee, M. Guchait, S. Raychaudhuri, and K. Sridhar, Phys. Rev. D **82**, 055006 (2010).
[18] S. Gopalakrishna, T. Mandal, S. Mitra, and R. Tibrewala, Phys. Rev. D **84**, 055001 (2011); S. Gopalakrishna, T. Mandal, S. Mitra, and G. Moreau, J. High Energy Phys. 08 (2014) 079.
[19] A. Azatov, O. Bondu, A. Falkowski, M. Felcini, S. Gascon-Shotkin, D. K. Ghosh, G. Moreau, and S. Sekmen, Phys. Rev. D **85**, 115022 (2012).
[20] A. Girdhar, Pramana **81**, 975 (2013).
[21] L. Wang and X. F. Han, Phys. Rev. D **86**, 095007 (2012).
[22] N. Bonne and G. Moreau, Phys. Lett. B **717**, 409 (2012).
[23] Y. Okada and L. Panizzi, Adv. High Energy Phys. **2013**, 364936 (2013).
[24] S. Dawson, E. Furlan, and I. Lewis, Phys. Rev. D **87**, 014007 (2013).
[25] S. Dawson and E. Furlan, Phys. Rev. D **89**, 015012 (2014).
[26] ATLAS Collaboration, Phys. Lett. B **716**, 1 (2012).
[27] CMS Collaboration, Phys. Lett. B **716**, 30 (2012).
[28] B. Mukhopadhyaya and S. Nandi, Phys. Rev. Lett. **66**, 285 (1991).
[29] B. Mukhopadhyaya and S. Nandi, Phys. Lett. B **266**, 112 (1991).
[30] F. Abe *et al.* (CDF Collaboration), Phys. Rev. Lett. **80**, 2525 (1998).
[31] G. Abbiendi *et al.* (OPAL Collaboration), Phys. Lett. B **521**, 181 (2001).
[32] J. A. Aguilar-Saavedra, Phys. Rev. D **67**, 035003 (2003); Phys. Rev. D **69**, 099901(E) (2004).
[33] T. Aaltonen *et al.* (CDF Collaboration), Phys. Rev. Lett. **107**, 261801 (2011).
[34] T. Aaltonen *et al.* (CDF Collaboration), Phys. Rev. Lett. **106**, 141803 (2011).
[35] (ATLAS collaboration), Report No. ATLAS-CONF-2013-051.
[36] (ATLAS collaboration), Report No. ATLAS-CONF-2013-056.
[37] (ATLAS collaboration), Report No. ATLAS-CONF-2013-060.
[38] G. Aad *et al.* (ATLAS Collaboration), Phys. Lett. B **718**, 1284 (2013).
[39] G. Aad (ATLAS Collaboration), Phys. Rev. Lett. **108**, 261802 (2012).
[40] S. Chatrchyan (CMS Collaboration), Phys. Rev. Lett. **107**, 271802 (2011).
[41] S. Chatrchyan *et al.* (CMS Collaboration), Phys. Lett. B **729**, 149 (2014).
[42] F. J. Botella, G. C. Branco, and M. Nebot, J. High Energy Phys. 12 (2012) 040.
[43] M. Aoki, E. Asakawa, M. Nagashima, N. Oshimo, and A. Sugamoto, Phys. Lett. B **487**, 321 (2000).
[44] M. Aoki, G. C. Cho, M. Nagashima, and N. Oshimo, Phys. Rev. D **64**, 117305 (2001).
[45] A. Pukhov *et al.*, arXiv:hep-ph/9908288.
[46] M. L. Mangano, M. Moretti, F. Piccinini, R. Pittau, and A. D. Polosa, J. High Energy Phys. 07 (2003) 001.
[47] T. Sjostrand, S. Mrenna, and P. Z. Skands, J. High Energy Phys. 05 (2006) 026.
[48] A. S. Belyaev *et al.*, arXiv:hep-ph/0101232.
[49] M. L. Mangano, M. Moretti, F. Piccinini, and M. Treccani, J. High Energy Phys. 01 (2007) 013.
[50] M. Cacciari, G. P. Salam, and G. Soyez, Eur. Phys. J. C **72**, 1896 (2012).